Swansea University
Prifysgol Abertawe

Cronfa
Setting Research Free

Cronfa - Swansea University Open Access Repository

This is an author produced version of a paper published in :
Agricultural and Forest Meteorology

Cronfa URL for this paper:
http://cronfa.swan.ac.uk/Record/cronfa20823

Paper:
Alton, P. (2014). Reconciling simulations of seasonal carbon flux and soil water with observations using tap roots and hydraulic redistribution: A multi-biome FLUXNET study. *Agricultural and Forest Meteorology, 198-199*, 309-319.

http://dx.doi.org/10.1016/j.agrformet.2014.08.019

This article is brought to you by Swansea University. Any person downloading material is agreeing to abide by the terms of the repository licence. Authors are personally responsible for adhering to publisher restrictions or conditions. When uploading content they are required to comply with their publisher agreement and the SHERPA RoMEO database to judge whether or not it is copyright safe to add this version of the paper to this repository.
http://www.swansea.ac.uk/iss/researchsupport/cronfa-support/

Reconciling simulations of seasonal carbon flux and soil water with observations using tap roots and hydraulic redistribution; a multi-biome FLUXNET study

Paul B. Alton, Geography Dept., Swansea University, SA2 8PP, UK.

p.alton@swansea.ac.uk +44(0)1792 295069

July 16, 2014

1 Abstract

Understanding the response of plants to soil moisture stress is important given a future climate subject to greater extremes, including drought. Nevertheless, major discrepancies still exist between observed and simulated seasonal carbon, water and energy fluxes at the vegetated land-surface. For tropical forest, these discrepancies have been reduced, especially during the dry season, by taking account of tap roots and hydraulic redistribution. The expanding FLUXNET open-access archive allows the current study to extend the investigation of seasonal drought-stress to ten different vegetation types. A state-of-the-art land-surface model is enhanced to take account of tap roots and hydraulic redistribution in order to compare with traditional simulations. Carbon fluxes and fractional soil water content are simulated and compared against observations. We find that a traditional approach, by neglecting tap roots, simulates a seasonal drought for trees and shrubs which is generally too severe compared to observed net carbon flux. The introduction of a tap root benefits tropical broadleaf forest and other ecosystems with high annual potential evapotranspiration in reducing observation-model discrepancies. Our simulations suggest a minor role for hydraulic redistribution, modifying weekly soil moisture rather than substantially changing seasonal water flux totals.

Keywords

carbon cycle; water cycle; land-surface modelling, Moderate Resolution Imaging Spectroradiometer (MODIS); FLUXNET; plant functional types; drought

2 Introduction

Assessing the resilience of plants to soil moisture stress and seasonal drought is not only important for understanding ecosystem functioning and its role within the carbon cycle. The feedback of water and heat fluxes from vegetation to the atmosphere can change regional climate, surface temperature and land-surface cover (Denman et al. 2007; Richardson et al. 2013) and is key to predicting the response of a future biosphere subject to greater climatic extremes (Fischer & Schär 2010).

Nevertheless, major discrepancies still exist between observed and simulated seasonal carbon, water and energy fluxes at the vegetated land-surface. For example, standard land-surface models (LSMs) predict a drought-induced reduction in both ecosystem carbon assimilation and evapotranspiration during the tropical dry season (Baker et al. (2008). In contrast, FLUXNET observations at one tropical forest reveal a 25% *increase* in evapotranspiration and sustained ecosystem carbon assimilation during this period (Goulden et al. 1996; Da Rocha et al. 2004). Examining a number of factors, Baker et al. (2008) conclude that access to deep (>3.5 m) soil water via tap roots is important to sustain gross productivity during the tropical dry season, although a simultaneous moisture-limited reduction in heterotrophic respiration is also implicated. Likewise, growing season evapotranspiration at four Californian FLUXNET sites simulated by Ichii et al. (2009) is reconciled with observations by the introduction of roots that are much deeper (e.g. 4 m for needleleaf forest) than values measured in the literature. This latter study, whilst thought-provoking, is based on a bucket model (single soil layer, no baseflow and linear root distribution) which is much simpler than the soil and plant hydrology adopted in most LSMs. Nevertheless, the aforementioned studies suggest our understanding of plant hydrology is incomplete, or at the very least poorly formulated in LSMs, and that plants might be more resilient to drought than has been hitherto supposed.

Deep roots have been excavated in the tropics and are believed to play an important role in drought-avoidance (Nepstad et al. 1994). Outside the tropics, 2-5 m tap roots are recorded at some boreal and mediterranean sites (Dawson & Pate 1996). However, the prevalence and importance of tap roots amongst different Plant Functional Types (PFTs) is not well established. (Acronyms and abbreviations used in the text are listed in Tab. 1). Compilations of multibiome measurements reveal that vast majority of root biomass lies in the upper metre (Jackson et al. 1996). Schenk & Jackson (2005) estimate that only 10% of global vegetation has >5% of root biomass deeper than 2 m, deep roots being most likely in seasonal (sub-)tropics for medium

texture soils. Even for trees, the majority of roots are constrained to the near-surface layers to allow competitive nutrient recycling. Shallow rooting appears to be even more prevalent in grassland (Oliveira et al. (2005); Jipp et al. (1998)). For example, Puecheta et al. (2004) record a scale depth of only 0.12 m in temperate grassland.

Lee et al. (2005) argue that, given the small fraction of root biomass in deep tap roots, another mechanism must operate in order to sustain photosynthesis and evapotranspiration during the dry season. They claim that water from the lower, moist soil layers is redistributed to upper, drier soil layers in a process known as Hydraulic Redistribution (HR). HR operates via the root system, occurs mostly at night and potentially allows water to move more quickly through the soil profile compared to standard Darcian flow. Estimates of HR and its importance vary. One model simulation predicts that 20% of Amazonian evapotranspiration originates from HR (Lee et al. 2005). However, noctural recharge of the upper soil layers measured at one tropical broadleaf site indicates that only 10% evapotranspiration is provided by HR (Da Rocha et al. 2004). Sap flow measurements in arid savanna suggest that $\sim$10% of annual transpiration is supplied by HR (Scott et al. 2008). However, a simulation for arid shrubland predicts that HR supplies only 4% of total transpiration (Ryel et al. 2002).

The expansion of the FLUXNET open access database allows a more extensive investigation into the prevalence of tap roots and HR across many global PFTs and how their implementation into standard LSMs may reduce discrepancy between modelled and observed carbon fluxes. This may also relate to the long-standing enigma that standard LSMs systematically underestimate fractional soil water content (SWC) in the upper soil profile by 0.05-0.10 over a wide range of PFTs (Guo and Dirmeyer (2006)). This underestimation could spuriously increase simulated drought-stress. The bearing of HR and tap roots on this problem is currently unknown.

This study modifies a state-of-the-art LSM to take account of tap roots and HR. The overarching goal is to compare revised simulations at 79 FLUXNET sites (482 siteyears and 10 vegetational types) against observed Net Ecosystem Exchange (NEE) and fractional SWC. Note that tap roots and HR have hitherto been implemented in only one or, at most, a few sites (e.g. Lee et al. 2005; Baker et al. 2008; Ichii et al. 2009). Further, the simultaneous analysis of fluxes and soil water has seldom been attempted in the

past, although the carbon and water cycles are strongly coupled through the process of photosynthesis and transpiration. In contrast to many previous studies, the current investigation also focuses on the ability of a state-of-the-art model to reproduce *seasonal* rather than diurnal fluxes and states. Our specific objectives are:

1. to determine whether the inability of a standard LSM to reproduce dry season NEE in the tropics extends to other PFTs or climate zones;
2. conversely, to identify PFTs where drought is evident in observed fluxes and may or may not be reproduced by the simulation;
3. to reduce observation-model discrepancies for both seasonal carbon flux and soil water by implementing ecophysiological and field-based modifications for tap root and HR hydrology.

3 Material and Methods

The methodology consists of 3 experiments: (1) a standard, default simulation with traditional, shallow roots based on average field measurements (Jackson et al. 1996); (2) as (1) but adding a tap root; and (3) as (2) but allowing for HR between soil layers. First, the LSM and its modification are introduced. Then the datasets are described which serve either as model input (parameterisation and forcing) or for validation (fluxes and soil water content). Finally, the modelling protocol is explained.

3.1 LSM and its Modification

The current study uses the Joint UK Land Environmental Simulator (JULES-SF) which is an enhanced version of the new UK Met.Office Surface Exchange Scheme (Cox et al. 1999). Key equations for JULES-SF are given in the Appendix of Alton & Bodin (2010) with the exception of a subsequent reformulation of plant maintenance respiration which is summarised below. In the following model overview we focus on changes made to below-ground plant hydrology for the purposes of this study.

JULES-SF takes account of diffuse and direct sunlight at multiple heights within the canopy and is one of most elaborate LSMs which operates globally in terms of light interception (Alton et al. 2007). The energy calculation central to JULES-SF is the standard Penman-Monteith approach (Monteith 1965), ensuring the balance of ingoing and outgoing energy fluxes at the land-surface. Photosynthesis is calculated separately

within each of 5 leaf layers according to a biochemical co-limitation model (Collatz et al. 1991), before summing to produce a canopy total. Leaf photosynthesis is linked to transpiration through a Ball-Berry stomatal model (Ball et al. 1987). Plant respiration depends on maintenance and growth terms (Ryan 1991). The former includes separate, additive terms for leaf and root respiration according to Q_{10} relationships based, respectively, on canopy and soil temperature (Law et al. 1999). Stem respiration depends on the ratio of stem-to-leaf nitrogen concentration (Cox et al. 1999; 2004). Surface albedo is estimated according to the two-stream approximation of Sellers et al. (1996).

Within JULES-SF, the soil is divided into 4 layers of thickness (top downwards) of 0.1, 0.25, 0.65, 2.0 m. The total soil column is therefore 3 m. In the standard simulation (JULES-def), plant water extraction depends on the exponential fine root distribution which declines rapidly with depth. The exponential scale-depths are taken as averages (d_{root}=0.1-0.3 m) from Jackson et al. (1996) who collate and average measurements for a wide range of PFTs. Most LSMs possess a similar shallow rooting depth although sometimes a bucket model is adopted in which a single soil layer defines the maximum depth to which the linear, rather than exponential, rootstock extends (e.g. Ichii et al. 2009).

In the second experiment, we add a single tap root to the standard model (JULES-tap). This tap root is placed within the lowest soil layer (depth 1-3 m). There are few measurements of the partitioning of biomass between shallow root stock and tap roots which can be used directly to parameterise our model. From numerous compiled measurements, Jackson et al. (1996) estimate that root biomass below 1 m ranges from <1% in tundra to 8-9% in deserts and temperate needleleaf forest, with a median across all 11 biomes of only 2%. From a similar compilation, Schenk & Jackson (2005) estimate that only 10% global vegetation has >5% of root biomass deeper than 2 m. However, for broadleaf trees in a mediterranean climate, 17% of total root biomass is found at depths of 0.9m (Kurz-Besson et al. 2006). Further, nearly one third of roots have been found below 2 m from excavations at one tropical forest (Nepstad et al. 1994; Jackson et al. 1996). In order to assess the maximum impact of deep rooting we adopt a high value for the fraction of tap biomass (1/3).

The properties of roots (specific hydraulic conductivity, diameter, length etc) differ considerably between shallow rootstock and deep tap roots (McElrone et al. 2004). However, these kind of detailed and differen-

tiated properties are not yet formulated explicitly in JULES-SF or any other global LSM. Extraction from each soil layer depends simply on the fraction of total root mass (shallow plus tap) present in that layer. This Ohm's Law analogy to root conductance (Tyree & Ewers 1991; Sellers et al 1996), which is also adopted below for HR (see Eq. 1 in Appendix), is a necessary simplification but one that we examine critically in the Results.

In the third experiment, we modify JULES-tap to allow for transport of water from wetter to drier soil layers *via* the root system (JULES-tap-HR). This hydraulic redistribution is in addition to the bulk Darcian soil flow present in all LSMs. The formulation of HR is based on Lee et al. (2005) and is described in detail in the Appendix. Note that HR can be either upwards or downwards according to whether the upper soil layers are subject to drought or heavy precipitation. We assume HR only takes place at night since transpiration is expected to drive water transport in the roots during the daytime.

For all 3 experiments, the moisture content within each soil layer is determined as the balance between water input (precipitation) and water output. The latter consists of evapotranspiration (i.e. soil and canopy evaporation as well as transpiration) and runoff (both above and below-ground). The below-ground runoff or baseflow is missing in bucket models but present in most standard LSMs. The model can store water in the soil (ΔSMC), on top of the soil surface as snow (ΔSNOW) and on the surface of canopy leaves (ΔCAN). ΔCAN relates linearly to LAI. Both ΔSNOW and ΔCAN are small compared to ΔSMC. Fig. 1 given an overview of model hydrology and the key water-balance equation.

The model contains 10 PFTs defined in Tab. 2. Based on site description, each FLUXNET location is attributed to one of these PFTs and simulations are conducted separately for each site.

3.2 Datasets

As described separately below, datasets serve either as model input or as validation of model output.

3.2.1 Model Input

As input, JULES-SF requires biophysical parameter values, meteorological forcing and a Leaf Area Index (LAI) timeseries or phenology. Many of the biophysical parameters are PFT-specific and include plant

attributes which are either structural (e.g. rooting depth, canopy height), optical (e.g. leaf absorptance) or physiological (e.g. photosynthetic capacity, minimum stomatal conductance). They are assigned using average collated field measurements (Alton & Bodin 2010). For the most influential parameter on modelled carbon fluxes, photosynthetic capacity (V^0_{cmax}), we adopt the mean of Wright et al. (2004) and Kattge et al. (2009), weighting for the number of measurements for each PFT. Before doing so, we convert the measurements of leaf nitrogen collated by Wright et al. (2004) into estimates of V^0_{cmax} using the same procedure as Kattge et al. (2009). Although there may be overlap in measurements contained in Wright et al. (2004) and Kattge et al. (2009), removing duplicates from such large samples is beyond the scope of the present study. Furthermore, our approach yields measured V^0_{cmax} averages per PFT which agree well with values retrieved in calibration experiments (Alton 2011). It is often advantageous to tune parameters such as V^0_{cmax} to each site or at least for each PFT as part of the model calibration. However, the current study tests the impact of model changes and, hypothetically, a separate calibration in each experiment could offset differences producted by reformulation of the model. Therefore, for the current investigation, we adopt constant values for each PFT based on the best average measurements available in the literature. Average soil composition measured at each site is taken from the FLUXNET ancillary database (Agarwal 2012). Recorded clay and silt contents determine soil hydraulic properties (e.g. conductance at saturation, Clapp-Hornberger exponent) based on the soil categorisation in Campbell & Norman (1998).

Model forcing consists of standard meteorological variables and LAI. Site meteorology is provided in the FLUXNET database and this is averaged to the 3-hourly model timestep. Although the FLUXNET meteorology is gap-filled (Falge et al. 2002), some siteyears contain a hiatus e.g. in winter. We fill these extended gaps with the Princeton global reconstructed climatology (Sheffield et al. 2006) using the 3-hourly meteorology within the corresponding 1° grid square. This allows the model to simulate total *annual* fluxes where necessary. However, our focus is the growing season for which the tower-based site meteorology is usually fairly complete. The main model calculation (Penman energy balance and simulation of sites fluxes) is 3-hourly, consistent with the Princeton forcing used to fill extended gaps in the site meteorology. This also provides sufficient temporal resolution to simulate precipitation infiltration and Darcian flow in the soil. However, HR allows for faster moisture transfer and we modify the model so that it updates moisture in the soil layers on a half-hourly basis. This is an internal ministep which does not increase the overall computational burden significantly (an important consideration in a model that is normally run globally)

but provides additional numerical stability in the calculation of water balance when HR is occurring rapidly.

For LAI, we adopt the Collection 5 MODIS MCD15A2 product (Schaaf et al. 2002). A 7km×7km subset (49 pixels) centred on the site location is used to mean average pixels of good quality (i.e. main algorithm, no significant cloud and >50% detectors working; Yang et al. 2006). The satellite phenology is normalised to maximum *in situ* LAI where available (2/3 of sites). MODIS data are only available from 2002. For earlier siteyears (one third of sample), we create a satellite phenology based on the median value acquired for the same day-of-year over the period 2002-2008. The error introduced by this approximation is small compared to other model errors stemming from, for example, parameter calibration.

3.2.2 Validation

To validate model output we compare against NEE, SWC and, to a lesser extent, latent heat flux (LE), all recorded in the main FLUXNET database. Measurements are available to the general modelling community for 79 sites and encompass 482 siteyears between 1991-2010, though the bulk (93%) range 1997-2009 (Falge et al. 2002; Yuan et al. 2010). Sites are distributed worldwide but are biassed towards forest in North America and Europe. To minimise the impact of incomplete energy closure (Foken 2008), we exclude fluxes recorded under low frictional velocity (<0.16 ms^{-1}; Goulden et al. 1996; Reichstein et al. 2003) or, if frictional velocity is unrecorded, where windspeed <2 ms^{-1} (Medlyn et al. 2003). To compare with model output, good quality observed NEE is averaged over a 3hr interval in the first instance, although much of our seasonal analysis relies on weekly averages of both modelled and observed fluxes, as discussed in the Results.

SWC is measured at an average depth of 8 cm (SWC1) and 19 cm (SWC2). Coverage is quite low. Thus, SWC1 and SWC2 are only available for, respectively, 46% and 32% of the eddy covariance fluxes. No valid measurements are available for tundra, shrubs and C4 crops. To filter out spurious (unreasonable) observations, we reject the 1% of SWC1 and SWC2 values in excess of 0.55.

Tab. 2 shows the number of sites per PFT whilst Tab. 3 summarises the main datasets.

3.3 Modelling Protocol

A simulation is conducted for each site using JULES-def, JULES-tap and JULES-tap-HR. Model soil moisture is spun-up by a 3yr pre-simulation using the site meteorology placed back-to-back where necessary (<3 siteyears available). Initially, the model is validated against seasonal moisture content and, to that end, both modelled and observed NEE and SWC are averaged over weekly bins.

For most sites, SWC1 and SWC2 do not provide sufficient coverage either in time or depth to reconstruct seasonal total soil moisture content (SMC in kg m^{-2}). Therefore, we sought a proxy for total SMC or soil moisture stress. We explored the MODIS mid-infrared to near-infrared reflectance ratio (Ceccato et al. 2001; Cheng et al. 2006) and the evaporative fraction ratio, the latter based on observed sensible and latent heat fluxes (Schwalm et al. 2010). However, both ratios correlate strongly with LAI (R^2=0.07-0.44 and R^2=0.35-0.86, respectively; $p<0.01$) making them unreliable as proxies. Both Zhao & Running (2010) and Angert et al. (2005) rely on the Palmer Drought Index but this is a modelled variable using a bucket approach to soil water balance. Reichstein et al. (2007) define an index of water availability as the ratio of actual evapotranspiration to potential evapotranspiration. However, as the authors themselves admit, this index does not isolate the limitation by water availability since actual evapotranspiration, though measured, depends on LAI. Furthermore, potential evapotranspiration is partly modelled. To compare moisture stress in a range of LSMs, Guo & Dirmeyer (2006) use simulated Plant Available Water (PAW) defined as the difference between current soil moisture content and the plant wilting point. In lieu of a suitable observed variable, we adopt a dual approach to broaden our perspective. Firstly, we examine NEE (measured fluxes) against simulated fractional Soil Water Content (SWC) across the total soil column. Then, we examine Gross Primary Product (GPP; derived from fluxes) against simulated PAW for the total soil column. GPP is derived as R_E - NEE where R_E is the ecosystem respiration, which is modelled separately for each sitemonth as a quadratic function of air temperature and best-fit to observed nighttime NEE (Medlyn et al. 2003). The PAW is derived assuming a wilting point of -4 MPa in soil water potential.

4 Results and Discussion

4.1 Carbon fluxes

In Figs. 2 and 3, we plot modelled and observed NEE against the deficit in fractional SWC (ΔSWC) for the default model (JULES-def) and the tap root model (JULES-tap), respectively. To separate the approximate seasonal change in peak carbon assimilation and respiration, NEE is shown separately for canopy light saturation (shortwave irradiance >300 Wm^{-2}; NEE(sat)) and for nighttime (NEE(night)). A similar approach has been adopted by previous authors (e.g. Goulden et al. 2004) who wish to focus on measured (NEE) rather than derived (e.g. GPP) fluxes. Observation minus model differences in NEE under light-saturation, ΔNEE(sat), correlate inversely and strongly with observation minus model differences in LE under light-saturation, ΔLE(sat) (ΔNEE(sat)[μmol m^{-2} s^{-1}]=-0.12ΔLE(sat)[Wm^{-2}]-2.9; R^2=0.64; $p<0.001$), suggesting that both are driven by the same process (photosynthesis and transpiration).

Focusing firstly on measurements for trees and shrubs, observed NEE(sat) is largely neutral with respect to increasing seasonal soil moisture deficit (Fig.2). However, there is an increase in NEE(sat) for natural grass. For C3 grass this may be partly attributable to increased seasonal ecosystem respiration, which is reflected in increasing NEE(night). Expressing carbon fluxes as GPP against PAW provides a somewhat different perspective (Fig. 4). There is a steady decrease in GPP as PAW is reduced, the decline being gentle for broadleaf trees but somewhat steeper for needleleaf trees. For mediterranean needleleaf trees there appears to be an inconsistency between Fig.2 and Fig. 4. On closer inspection, we find that PAW is more sensitive than ΔSWC to soil type and its assumed properties (for example, the wilting point differs quite a lot between sand or loam soils) and this tends to produce steeper gradients across the dependent variable. Fig. 4 shows the role of the tap root in sustaining GPP to lower PAW, at least for broadleaf and tropical broadleaf trees. However, there is often an offset present e.g. for shrubs and tropical broadleaf, possibly owing to an absence of model calibration in the current study.

Both Schwalm et al. (2010) and Reichstein et al. (2007) claim a drop in gross productivity under drought. However, both these studies are based on annual fluxes, either comparing sites for different climate zones or comparing several years for the same site. Relative few studies quantify the response *across* the season for the same site or PFT under changing soil moisture deficit. For a temperate deciduous broadleaf forest,

Wilson & Baldocchi (2000) claim to detect the onset of seasonal drought in both the ratio of measured sensible and latent heat and the inferred surface conductance. However, both these quantities are sensitive to LAI and the seasonal response is therefore convoluted by phenology. Likewise, Fig. 2 cannot be purely interpreted as a response to soil moisture stress. For example, the concomitant change in average LAI with ΔSMC is strong for crops. Furthermore, crop phenologies recorded *in situ* and by satellite often match poorly owing to the mosaic of vegetation covered by the satellite footprint. This gives rise to large differences between observed and modelled NEE(sat) for C3 crops (Cr3) in Fig. 2 since the model is primarily driven by satellite (MODIS) phenology.

Reichstein et al. (2003) infer a reduction in seasonal photosynthetic capacity from eddy covariance fluxes recorded at 3 mediterranean sites, comprising two forests and one shrubland. However, this drought stress is only detected at very low soil moisture (SWC$\sim$0.07) which occurs only infrequently at most of our sites ($\leq$6% of measurements; see panel (a) of Fig. 7, which is discussed in detail below in §4.2). For the dry season within a tropical broadleaf forest, Goulden et al. (2004) measure a small systematic decrease in ecosystem respiration (2 μmol m^{-2} s^{-1}) and a gross productivity which is either sustained or increasing owing to access to deep (10 m) water (Baker et al. 2008).

Our results are somewhat ambiguous according to how we define soil moisture status (ΔSWC or PAW). However, for trees and shrubs, there is an apparent absence of stress on observed NEE at light saturation over a large range of soil moisture conditions (Fig. 2) and a generally gentle decline in GPP. In contrast, NEE(sat) simulated by the default model exhibits an increase with soil moisture deficit for most PFTs and a marked reduction in GPP. Compared to the observations, the model is oversensitive to drought, particularly for trees and especially for tropical broadleaf forest. This behaviour is also reflected in the corresponding seasonal profiles for LE (not shown). In tropical broadleaf forest, for example, an increase in modelled NEE(sat) at ΔSWC$<$ -0.07 (reduction in carbon assimilation) is mirrored by a one third reduction in modelled LE at light saturation.

The implementation of a tap root yields a better match between model and observed NEE for trees and shrubs (Fig. 3; see also Tab. 4). It also produces a shallower gradient with respect to PAW and sustains GPP to lower PAW. This is particularly beneficial to simulations of tropical broadleaf forest. The deep root

allows plants to access water in the lowest soil layer (1-3 m) which would otherwise remain in the lower soil column or drain out of the system as baseflow runoff. With the tap root implemented, there is no obvious improvement for crops because of the limiting accuracy of phenology, discussed above. Furthermore, there is no obvious improvement for grassland (Fig. 2-4). Depth-resolved soil moisture measurements indicate that grass roots are short compared to trees (Oliveira et al. 2005; Jipp et al. 1998; Pucheta et al. 2004) and long-term eddy-covariance studies reveal that grassland gross productivity and ecosystem respiration are very sensitive to drought (Scott et al. 2010). Using compiled global root measurements, Schenk & Jackson (2005) claim that perennial herbs are five times less likely to be deeply rooted compared to shrubs and trees. For tropical broadleaf forest, some stress is still apparent in the model even after implementation of a tap root (Fig. 3).

With HR implemented, seasonal NEE does not differ significantly from Fig. 3 for JULES-tap (Tab. 4). As discussed below, the main impact of HR appears to be on weekly rather than seasonal timescales. Although HR can move water around the soil profile to irrigate roots in the drier layers, once water has been removed from the total soil column, either by evapotranspiration or baseflow, HR does little to alleviate soil moisture stress. Thus, HR acts to delay rather than to preclude drought-stress. Both the reduction in observation-model NEE discrepancies with tap root implementation and the largely neutral seasonal impact of HR are quantified in Tab. 4.

Although the improvement in model performance with tap root implementation depends to some extent on PFT (trees/shrubs versus grass), climate also plays important a role. Fig. 5 shows the change in Root Mean-Square Error (RMSE) between JULES-def and JULES-tap when sites are plotted against annual potential evapotranspiration. There is an improvement with tap root implementation (ΔRMSE decreasing) for sites experiencing a higher atmospheric demand for water (higher potential evapotranspiration). However, the systematic improvement is small (1 μmol m^{-2} s^{-1}) compared to the typical RMSE of the default simulation (4 μmol m^{-2} s^{-1}). High RMSE is caused by the large observational errors which characterise eddy covariance fluxes (1.5-3 μmol m^{-2} s^{-1}; Goulden et al. 1996; Medlyn et al. 2005). Furthermore, model bias is evident, even when drought stress is minimal (e.g. at ΔSWC=0 in Fig. 2 for tropical broadleaf forest), and our simulations (necessarily) use PFT averages for biophysical parameters such as photosynthetic capacity which are known to vary greatly even within PFTs (Wright et al. 2004). Somewhat surprisingly, inclusion

of annual precipitation into the water balance of Fig. 5 (e.g. potential evapotranspiration minus precipitation) does not yield a stronger relationship against ΔRMSE. However, the Princeton dataset providing our estimate of annual precipitation possesses only a coarse spatial resolution (∼100 km).

Given the influence of climate on the inferred presence of tap root, we re-run the JULES-tap simulation, allowing the fraction of tap root (with respect to total root biomass) to be optimised for each site. This is done using a gradient-based Levenberg-Marquardt search algorithm (Press et al. 1992) which minimises the χ^2 differences between observed and modelled fluxes i.e. $\chi^2 = \sum(obs - mod)^2/\sigma^2$ where σ is assumed to be 3 μmol m^{-2} s^{-1} and 30 W m^{-2} for NEE and LE, respectively (Goulden et al. 1996; Medlyn et al. 2005). The retrieved optimised values of tap root fraction exhibit a large range (Fig. 6). However, only a third of our sites have more than 5% in tap roots. Extrapolating from site measurements, Schenk & Jackson (2005) estimate that only 10% global vegetation has >5% of root biomass deeper than 2 m. Thus we might expect at least 10% of our sites to possess >5% of roots in the lowest JULES soil layer (i.e. deeper than 1 m). By far the PFT with the highest tap root fraction is tropical broadleaf forest (median value 0.4). This substantial fraction is approximately consistent with excavations at one tropical forest which reveal that one third of root biomass exists in deep roots (Nepstad et al. 1994; Jackson et al. 1996). Field measurements reveal that tap roots are present in 75% tropical trees (Canadell et al. 1996). Canadell et al (1996) compile the maximum rooting depth recorded in different biomes, rather than the proportion of root mass below 1 m appropriate for parameterisation/validation of our model. Notably, however, they find that the deepest roots are present in deserts (not covered by present study) and tropical biomes.

McElrone et al. (2004) measure a hydraulic conductivity which is 2.3-6.0 (mean 3.8) times higher in deep roots compared to shallow roots for broadleaf and needleleaf trees in an environment which is susceptible to seasonal drought. All else being equal, increasing tap root conductivity by a factor of 3.8 would reduce the optimised tap root fraction by the same factor owing to the Ohm's law analogy formulated in JULES (see Eq. 1 in the Appendix which shows how water flow for HR, which works in a similar way, is proportional to the product of conductance and root fraction). However, a factor 3.8 is likely to be the maximum reduction since the water path length is longer for tap roots compared to shallow roots (e.g. factor ∼2 in McElrone et al. 2004) which reduces the conductance for tap roots relative to shallow roots (conductance is proportional to the product of conductivity and path length; Tyree & Ewers 1991). In conclusion, our simulations

suggest that the tap root fraction could be as little as 11% for tropical broadleaf forest and even smaller for other PFTs. The minor fraction within tap roots explains, in part, why deep roots have been overlooked in standard LSMs despite their important function in relieving seasonal drought.

4.2 Soil moisture

Fig. 7 compares the fraction of soil water content at depths 8 cm and 19 cm (SWC1 and SWC2, respectively) for both the model and observations using the median average within weekly bins. A median is adopted to remove sensitive towards high precipitation events in the observations. Results are shown for JULES-tap and JULES-tap-HR only. The result for the default simulation is similar to JULES-tap because the tap root model extracts additional moisture from the lowest soil layer (depth 2.5 m) rather than from the upper soil profile pertaining to SWC1 and SWC2. On average, the fractional moisture observed in the lower soil level (SWC2) is 0.03 higher than the value measured in the upper layer (SWC1). The model has difficulty reproducing this offset especially with HR implemented. We investigated whether the observed offset was due to a vertical change in soil composition and associated hydraulic properties. However, there is no evidence of an increase in clay content with depth from the FLUXNET ancillary database (Agarwal 2012) which, if present, might give rise to greater holding capacity at lower soil depth.

For JULES-tap there is quite a lot of dispersion between SWC1 and SWC2. This is partly explained by clusters of points where the top soil layer has reached wilting point but moisture is still draining from the lower layer. In HR, this situation does not arise since the roots equilibrate soil moisture across the vertical soil layers. For the observations, the dispersion could be associated with the inherent diversity of soil hydraulic properties which are rather poorly known at individual sites and estimated in the model according to silt and clay content. Furthermore, the observations often provide only an instantaneous measurement that may fall either side of a heavy precipitation event, whereas the model averages all 3-hourly steps over the duration of a week.

It is difficult to determine which revised model (JULES-tap or JULES-tap-HR) performs better against the observations until the systematic offset between modelled and observed fractional SWC is removed and the full diversity of soil hydraulic properties is accounted for at all sites. The systematic offset is highlighted in

Fig. 8, where modelled SWC2 is compared against measurement throughout the year. For model output, only JULES-tap is shown. JULES-def exhibits a similar seasonal behaviour though slightly offset to lower values (i.e. away from the observations). JULES-tap-HR is very similar to JULES-tap (see also Tab. 4 which quantifies the RMSE for each simulation). Although the model often captures observed seasonal behaviour, on average it is too dry with respect to the observations, even with tap root and HR enhancements. This is a general problem of LSMs. A diverse range of models underestimate growing season fractional SWC in the top metre by a significant amount (0.05-0.10) when compared against measurements in forest, grassland and cropland (Guo & Dirmeyer 2006). Stöckli et al. (2008) implement a catchment-scale aquifer into the Community Land Model to allow for water storage below the 3.5 m soil layer and irrigation of the root-zone during drought. This novel enhancement significantly improves predicted LE at 15 FLUXNET sites but the simulated fractional SWC, whilst increased, still lies 0.05-0.10 below observed values during the driest part of the growing season. Furthermore, our simulations demonstrate that this offset is not eliminated by implementing tap roots or HR. Clearly more work is required to resolve this systematic offset using site-specific measurements of soil hydraulic properties, deep soil moisture (to monitor aquifer and tap root sources) and bedrock features (which may alter baseflow runoff).

When tap roots and HR are implemented together (JULES-tap-HR), there is an average increase in annual transpiration of 13% compared to shallow rooting. In a few cases, the additional transpiration is 100 mm which is significant. Most of the 13% increase comes from the tap root, with HR contributing a mere 2% to the annual total. HR seems to be more important on weekly (Fig. 7) rather than seasonal timescales.

Previous estimates of the importance of HR vary. Lee et al. (2005) simulate a 20% increase in annual evapotranspiration over Amazonia when HR is implemented although it is not clear how the roots are distributed in their model. Measured nocturnal recharge of the upper soil layers at one tropical broadleaf site, Tapajos, indicates that a maximum of 10% annual evapotranspiration is provided by HR (Da Rocha et al. 2004). Sap flow measurements in arid savanna suggest that $\sim$10% of annual transpiration is supplied by HR (Scott et al. 2008) although a simulation of HR within arid shrubland predicts that only 4% annual transpiration arises from HR (Ryel et al. 2002).

Some previous measurements and simulations suggest that HR could be important seasonally, at least in

combination with deep roots. Thus, isotope measurements within trees under a mediterranean climate indicate that a broad proportion of dry season transpiration (9-47%) originates from water lifted by deep roots (Dawson & Pate 1996). However, seasonally, our results suggest that it is the tap root, rather than nocturnal HR, which sustains carbon assimilation under soil moisture deficit (Figs. 2 and 3). Our simulations are rather insensitive to the parameter values adopted for HR. For example, a factor 2 increase in C_{sat} (Eq. 1 in Appendix), covering the range used for HR in the literature (Becker et al. 1999; Ryel et al. 2002; Lee et al 2005), only produces a change of 2% in annual transpiration. Our simulations also confirm one problem already noted by Lee et al. (2005), that HR can lead to overestimates of nighttime evaporation as transported water is lost from the upper soil layer rather than transpired next day. We believe that more depth-explicit site measurements of root distribution and soil moisture are required in order to formulate HR correctly in the model.

4.3 Limitations of Study

Although providing some initial insights into the role that deep roots and HR could play in land-surface modelling, our study has significant limitations:

1. Dawson & Pate (1996) distinguish lateral, shallow, nutrient-acquiring fine roots from stouter, sinker tap roots, both categories having different hydraulic conductivities and efficiencies. Although we endeavour to account for some of these differences when estimating the tap root fraction, our experiment is necessarily a simple first step in representing dimorphic root systems in global LSMs;

2. Although inclusion of deep roots generally appears to improve simulations of seasonal NEE in trees and shrubs, we cannot exclude the possibility that other model enhancements could produce a similar effect (e.g. accounting for seasonal change in V^0_{cmax}). However, we know that deep roots are found in the field and that they are neglected in the vast majority of LSMs. Moreover, any seasonal increase in V^0_{cmax} implies greater transpiration which requires better access to deep soil water (via tap roots);

3. Ultimately, in order to be useful to global simulations, we have analysed our sites according to PFT. However, within any given PFT, extraction from different parts of the soil profile may relate to life strategy (e.g. deciduous-evergreen habit) of individual species (Jackson et al. 1995).

5 Summary and Conclusions

The current study investigates the prevalence of seasonal drought across 79 FLUXNET sites (482 siteyears) using a state-of-the-art land-surface model, JULES-SF, enhanced to take account of tap roots and hydraulic redistribution. We examine both carbon flux and fractional soil water content across a wide range of plant functional types. Our most important findings are as follows:

1. Although somewhat sensitive to how we represent soil moisture deficit, the seasonal drought-stress inferred from observed carbon fluxes is less severe for trees and shrubs than that simulated by a traditional model using shallow rooting. The simulated drought-stress is reduced considerably by implementation of a 2 m tap root.

2. The prevalence of deep roots also depends on climate. Sites with high potential evapotranspiration rates appear to benefit most from the introduction of a tap root. A Levenberg-Marquardt optimisation of the model suggests that only one third of our sites possess >5% root biomass within tap roots. Tap roots appear most important in tropical broadleaf forest (40% root biomass). Note, however, that assuming an enhanced hydraulic conductivity for deep roots, these tap root fractions could be as much as four times lower i.e. a minor fraction of root biomass, which partly explains their neglect in standard LSMs despite their important function.

3. The model simulates quite well the seasonal change in fractional soil water content. However, as with other land-surface models, the current model, even with tap root and hydraulic redistribution enhancements, is too dry with respect to the observations. This systematic offset makes it difficult to establish whether the model performs better with hydraulic redistribution or not. In any case, hydraulic redistribution appears to have more impact on weekly soil moisture rather than seasonal totals. Thus, it is the tap root rather than hydraulic redistribution which extracts efficiently from the deeper (1-3 m) soil layers, yielding an average increase in annual transpiration of 10% compared to traditional shallow rooting.

6 Appendix

Hydraulic Redistribution (HR) is based on Lee et al. (2005). Thus, HR water flux (kg m^{-2} s^{-1}) is defined as:

$$Q = -C_{sat}\frac{r\Delta\psi}{1 + exp[0.02(\psi_{crit} - \psi)]} \quad (1)$$

where C_{sat} (kg m^{-3} s^{-1}) is the root hydraulic conductance when the soil column is saturated. A value of $2.5 \times 10^{-6} LAI_{max}$ is adopted for C_{sat} (Becker et al. (1999); Ryel et al. (2002)), where LAI_{max} is the maximum Leaf Area Index (m^2 m^{-2}) during the year. In Eq. 1, r is the root fraction in the uptake layer, $\Delta\psi$ (m) is the difference in soil water potential between the uptake (wet) and release (dry) layers. The denominator is a stress function which describes the steep reduction observed in water transport via the roots once soil water potential in the uptake layer (ψ in m) falls below a critical value ψ_{crit} (-200m; Sellers et al. 1996). HR constitutes a low-resistance conduit, relative to the bulk soil Darcian flow, between dry and wet soil layers.

Acknowledgements

We are grateful to the PIs and Co-Is of FLUXNET who make their data freely available to the ecological modelling community through the FLUXNET archive(http://FLUXNET.ornl.gov/). These contributors include, but are not limited to, Falge, E., M. Aubinet, P. Bakwin, D. Baldocchi, P. Berbigier, C. Bernhofer, A. Black, R. Ceulemans, A. Dolman, A. Goldstein, M. Goulden, A. Granier, D. Hollinger, P. Jarvis, N. Jensen, K. Pilegaard, G. Katul, P. Kyaw Tha Paw, B. Law, A. Lindroth, D. Loustau, Y. Mahli, R. Monson, P.Moncrieff, E. Moors, W. Munger, T. Meyers, W. Oechel, E. Schulze, H. Thorgeirsson, J. Tenhunen, R. Valentini, S. Verma, T. Vesala, and S. Wofsy.

References

Agarwal, D., (ed.) 2012 Biological and Ancillary Data for FLUXNET sites. Data set. Available on-line [http://www.fluxdata.org]

Alton, P, Ellis, R., Los, S., North, P. (2007) Improved global simulations of Gross Primary Product based on a separate and explicit treatment of diffuse and direct sunlight. *JGR*, 112, D07203

Alton, P. and Bodin, P. (2010) A comparative study of a multilayer and a productivity (light-use) efficiency land-surface model over different temporal scales *Agricultural and Forest Meteorology*, 150, 182-195

Alton, P., (2011) How useful are plant functional types in global simulations of the carbon, water and energy cycles? *JGR*, 116, G01030

Angert, A., Biraud, S., Bonfils, C., Henning, C., Buermann, W., Pinzon, J., Tucker, C., Fung, I. (2005) Drier summers cancel out the CO2 uptake enhancement induced by warmer springs *PNAS*, 102, 10823-10827

Baker, I.T., Prihodko, L., Denning, A.S., Goulden, M., Miller, S., da Rocha, H.R., (2008) Seasonal drought stress in the Amazon: reconciling models and observations. *J.Geophys. Res.* 113, G00B01, doi:10.1029/2007JG000644.

Ball, J., Woodrow, E., Berry, J. (1987) A model predicting stomatal conductance and its contribution to the control of photosynthesis under different environmental conditions *In* Progress in Photosynthesis Research Ed. Biggins, J., Nijhoff, M., 221-224, *Dordrecht, Netherlands*

Becker, P., Tyree, M., Tsuda, M., (1999) Hydraulic conductances of angiosperms versus conifers: similar transport sufficiency at whole-plant level *Tree Physiology*, 19, 445-452

Campbell, B. and Norman, J. (1998) Environmental Biophysics *Ed. Springer-Verlag, New York*

Canadell, J, RB Jackson, JR Ehleringer, HA Mooney, OE Sala, E-D Schulze. (1996) Maximum rooting

depth of vegetation types at the global scale. *Oecologia* 108:583-595

Ceccato, P., Flasse, S., Tarantola, S., Jacquemoud, S., Gregoire, J-M. (2001) Detecting vegetation leaf water content using reflectance in the optical domain *Remote Sensing of Environment*, 77, 22-33

Cheng, Y-B., Zarco-Tejada, P., Riano, D., Rueda, C., Ustin, S., (2006) Estimating vegetation water content with hyperspectral data for different canopy scenarios: relationships between AVIRIS and MODIS indices *Remote Sensing of Environment*, 105, 354-366

Collatz, G., Ball, J., Grivet, C., Berry, J. (1991) Physiological and environmental regulation of stomatal conductance, photosynthesis and transpiration: a model that includes laminar boundary layer *Agric.For.Meteorol.* 54, 107-136

Cox, P., Betts, R., Bunton, C., Essery, R., Rowntree, P., Smith, J. (1999) The impact of new land surface physics on the GCM simulation of climate and climate sensitivity *J.Climate Dynamics* 15, 183-203

Cox, P., Betts, R., Collins, M., Harris, P., Huntingford, C., Jones, C., (2004) Amazonian forest dieback under climate-carbon cycle projections for the 21st century *Theoretical and Applied Climatology*, 78, 137-156

Da Rocha, H., Goulden, M., Miller, S., Menton, M., Pinto, L., Freitas, H., Figueira, A. (2004) Seasonality of water and heat fluxes over a tropical forest in Eastern Amazonia *Ecological Applications*, 14, S22-S32

Dawson, T., Pate, J., (1996) Seasonal water uptake and movement in root systems of Australian phraeatophytic plants of dimorphic root morphology: a stable isotope investigation *Oecologia*, 107, 13-20

Denman, K.L., G. Brasseur, A. Chidthaisong, P. Ciais, P.M. Cox, R.E. Dickinson, D. Hauglustaine, C. Heinze, E. Holland, D. Jacob, U. Lohmann, S Ramachandran, P.L. da Silva Dias, S.C. Wofsy and X. Zhang, 2007: Couplings Between Changes in the Climate System and Biogeochemistry. In: Climate Change 2007: The Physical Science Basis. Contribution of Working Group I to the Fourth Assessment Report of the Intergovernmental Panel on Climate Change [Solomon, S., D. Qin, M. Manning, Z. Chen, M. Marquis, K.B.

Averyt, M.Tignor and H.L. Miller (eds.)]. Cambridge University Press, Cambridge, United Kingdom and New York, NY, USA.

Dirmeyer, P., Dolman, A., Sato, N. (1999) The global soil wetness project; a pilot project for global land surface modelling and validation *Bull.Amer.Meteor.Soc.* 80, 851-878 [http://www.iges.org/gswp/]

Falge, E., Tenhunen, J., Baldocchi, D., Aubinet, M., Bakwin, P., Berbigier, P., Bernhofer, C., Bonnefond, J-M., Burba, G., Clement, R., Davis, K., Elbers, J., Falk, M., Goldstein, A., Grelle, A., Granier, A., Gruenwald, T., Guomundsson, J., Hollinger, D., Janssens, I., Keronen, P., Kowalski., A., Katul, G., Law, B., Malhi, Y., Meyers, T., Monson, R., Moors, E., Munger, J., Oechel, W., Kyaw Tha Paw, U., Pilegaard, K., Rannik, U., Rebmann, C., Suyker, A., Thorgeirsson, H., Tirone, G., Turnipseed, A., Wilson, K., Wofsy, S. (2002) Phase and amplitude of ecosystem carbon release and uptake potential as derived from FLUXNET measurements *Agricultural and Forest Meteorology*, 113, 75-95

Fischer, E., Schär, C., (2010) Consistent geographical patterns of changes in high-impact European heatwaves *Nature Geoscience*, 3, 398-403

Foken, T. (2008) The energy balance closure problem – an overview *Ecological Applications*, 18, 1351-1367

Goulden M., Munger, J., Fan, S., Daube, B., Wofsy, S. (1996) Measurements of carbon sequestration by long-term eddy covariance: methods and a critical evaluation of accuracy *Global Change Biology* 2, 169-182

Goulden, M., Miller, S., da Rocha, H., Menton, M., de Freitas, H., Figueira, A., Sousa, C., (2004) Diel and seasonal patterns of tropical forest CO2 exchange

Guo, Z., Dirmeyer, P., (2006) Evaluation of the second Global Soil Wetness Project soil moisture simulations: 1. Intermodel comparison *JGR* 111, D22S02

Ichii, K. Wang, W., Hashimoto, H., Yang, F., Votava, P., Michaelis, A., Nemani, R., (2009) Refinement of rooting depths using satellite-based evapotranspiration seasonality for ecosystem modeling in California

588 *Agricultural and Forest Meteorology*, 149 1907-1918

589

590 Jackson, R., Cavelier, J., Goldstein, G., Meinzer, F., Holbrook, N., (1995) *Oecologia*, 101, 197-203

591

592 Jackson, R., Canadell, J., Ehleringer, J., Mooney, H., Sala, O., Schulze, E. (1996) A global analysis of root
593 distributions for terrestrial biomes *Oecologia*, 108, 389-411

594

595 Jipp, P., Nepstad, D., Cassel, K., Reis de Carvalho, C., (1998) Deep soil moisture storage and transpiration
596 in forests and pastures of seasonally dry Amazonia *Climatic Change*, 39, 395-412

597

598 Kattge, J., Knorr, W., Raddatz, T., Wirth, C. (2009) Quantifying photosynthetic capacity and its relation-
599 ship to leaf nitrogen content for global-scale terrestrial biosphere models *Global Change Biology*, 15, 976-991

600

601 Kurz-Besson, C., Otieno, D., Lobo do Vale, R., Siegwolf, R., Schmidt, M., Herd, A., Nogueira, C., David, T.,
602 David, J., Tenhunen, J., Pereira, J., Chaves, M., (2006) Hydraulic lift in cork oak trees in a savannah-type
603 Mediterranean ecosystem and its contribution to the local water balance *Pland and Soil*, 282, 361-378

604

605 Lee, J., Oliveira, R., Dawson, T., Fung, I. (2005) Root functioning modifies seasonal climate *Proceedings of*
606 *the National Academy of Science*, 102, 17576-17581

607

608 McElrone, A., Pockman, W., Martinez-Vilalta, J., Jackson, R., (2004) Variation in xylem structure and
609 function in stems and roots of trees to 20m depth *New Phytologist*, 163, 507-517

610

611 Medlyn, B., Barrett, D., Landsberg, J., Sands, P., Clement, R. (2003) Conversion of canopy-intercepted
612 radiation to photosynthate: review of modelling approaches for regional scales *Functional Plant Biology* 30,
613 153-169

614

615 Medlyn, B., Robinson, A., Clement, R., McMurtie, E. (2005) On the validation of models of forest CO_2
616 exchange using eddy covariance data: some perils and pitfalls *Tree Physiology* 25, 839-857

617

618 Nepstad DC, Carvalho CJR, Davidson EA, Jipp PH, Lefebvre PA, Negreiros GH, da Silva ED, Stone TA,
619 Trumbore SE, Vieira S. (1994) The role of deep roots in the hydrological and carbon cycles of Amazonian
620 forests and pastures *Nature* 372: 666-669

621

622 Press, W., Teukolsky, S., Vetterling, W., Flannery, B. (1992) *Numerical Recipes: the Art of Scientific Com-*
623 *puting*, Cambridge University Press, Cambridge

624

625 Oliveira, R., Bezerra, L., Davidson, E., Pinto, F., Klink, C., Nepstad, D., Moreira, A., (2005) Deep root
626 function in soil water dynamics in cerrado savannas of central Brazil *Functional Ecology*, 19, 574-581

627

628 Reichstein, M., Tenhunen, J, Roupsard, O., Ourcival J.M., Rambal S., Miglietta F., Peressotti A., Pecchiari
629 M., Tirone G., Valentini R.(2003) Inverse Modelling of seasonal drought effects on canopy CO_2/H_2O ex-
630 change in three Mediterranean ecosystems *JGR* 108, D23, 4726

631

632 Reichstein, M., Papale, D., Valentini, R., Aubinet, M., Bernhofer, C., Knohl, A., Laurila, T., Lindroth, A.,
633 Moors, E., Pilegaard, K., Seufert, G., (2007) Determinants of terrestrial ecosystem carbon balance inferred
634 from European eddy covariance flux sites *Geophysical Research Letters*, 34, L01402

635

636 Richardson, A., Keenan, T., Migliavacca, M., Ryu, Y., Sonnentag, O., Toomey, M., (2013) Climate change,
637 phenology and phenological control of vegetation feedbacks to the climate system *Agricultural and Forest*
638 *Meteorology*, 169, 156-173

639

640 Ryel, R,. Caldwell, M., Yoder, C., Or, D., Leffler, A., (2002) Hydraulic redistribution in a stand of Artemisia
641 tridentata: evaluation of benefits to transpiration assessed with a simulation model *Oecologia*, 130, 173-184

642

643 Schaaf, C., Gao, F., Strahler, A., Lucht W., Li X.; Tsang T., Strugnell N.C., Zhang X., Jin Y., Muller J.-P.,
644 Lewis P., Barnsley M., Hobson P., Disney M., Roberts G., Dunderdale M., Doll C., d'Entremont R.P., Hu
645 B., Liang S., Privette J.L., Roy D. (2002) First operational BRDF, albedo and nadir reflectance products
646 from MODIS *Remote Sensing Environment*, 83, 135-148

647

Schenk, H., Jackson, R., (2005) Mapping the global distribution of deep roots in relation to climate and soil characteristics *Geoderma* 126, 129-140

Schwalm, C., Williams, C., Schaefer, K., Arneth, A., Bonal, D., Buchmann, N., Chen, J., Law, B., Lindroth, A., Luyssaert, S., Reichstein, M., Richardson, A., (2010) Assimilation exceeds respiration sensitivity to drought: a FLUXNET synthesis *Global Change Biology*, 16, 657-670

Scott, R., Cable, W., Hultine, K., (2008) The ecohydrologic significance of hydraulic redistribution in a semiarid savanna *Water Resources Research*, 44, W02440

Scott, R., Hamerlynck, E., Jenerette, G., Moran, M., Barron-Gafford, G. (2010) Carbon dioxide exchange in a semidesert grassland throught drought-induced vegetation change *Journal of Geophysical Research*, 115, G03026

Sellers, P., Randall, D., Collatz, G., et al. (1996) A revised land surface parameterization (SiB2) for atmospheric GCMs. Part I: Model formulation *Journal of Climate* 9, 676-705

Sheffield, J., G. Goteti, and E. Wood (2006), Development of a 50-year high-resolution global dataset of meteorological forcings for land surface modeling, *J. Clim.*, 19, 3088–3111

Sheffield, J., E. F. Wood, and M. L. Roderick, 2012: Little change in global drought over the past 60 years. *Nature*, 491, 435-438. doi:10.1038/nature11575

Stöckli, R., Lawerence, D., Niu, G., Oleson, K., Thornton, P., Yang, Z., Bonan, G., Denning, A., Running, S. (2008) Use of FLUXNET in the Community Land Model Development *JGR* 113, G01025

Tyree, M., Ewers, F., (1991) Tansley Review 34: The hydraulic architecture of trees and other woody plants *New Phytol.*, 119, 345-360

Wilson, K., Baldocchi, D., (2000) Seasonal and interannual variability of energy fluxes over a broadleaved

temperate deciduous forest in North America *Agricultural and Forest Meteorology*, 100, 1-18

Wright, I., Reich, P., Westoby, M., Ackerly DD, Baruch Z, Bongers F, Cavender-Bares J, Chapin T, Cornelissen JH, Diemer M, Flexas J, Garnier E, Groom PK, Gulias J, Hikosaka K, Lamont BB, Lee T, Lee W, Lusk C, Midgley JJ, Navas ML, Niinemets U, Oleksyn J, Osada N, Poorter H, Poot P, Prior L, Pyankov VI, Roumet C, Thomas SC, Tjoelker MG, Veneklaas EJ, Villar R. (2004) The worldwide leaf economics spectrum *Nature*, 428, 821-827

Yang, W, Shabanov, NV, Huang, D, Wang, W, Dickinson, RE, Nemani, RR, Knyazikhin, Y, Myneni, RB (2006b). Analysis of leaf area index products from combination of MODIS Terra and Aqua data. *Remote Sensing of Environment*, 104(3), 297-312

Yuan, W., et al. (2010) Global estimates of evapotranspiration and gross primary production based on MODIS and global meteorology data *Remote Sensing of Environment*, 114, 1416-1431

Zhao, M., Running, S., (2010) Drought-induced reduction in global terrestrial net primary production from 2000 to 2009 *Science*, 329, 940-943

Table 1: An alphabetical list of acronyms and abbreviations used in the main text. Units are given where appropriate.

	Definition
GPP	Gross Primary Product (μm m^{-2} s^{-1})
HR	Hydraulic Redistribution
JULES-SF	Joint UK land environmental simulator
LAI	Leaf Area Index (m^2 m^{-2})
LE	Latent Energy flux (W m^{-2})
LSM	Land Surface Model
MODIS	Moderate Resolution Imaging Spectroradiometer
NEE	Net Ecosystem Exchange (μm m^{-2} s^{-1})
PFT	Plant Functional Type
RMSE	Root Mean Square Error
SMC	Soil Moisture Content (kg m^{-2})
SWC	fractional Soil Water Content (-)

Table 2: Plant functional types examined in the current study with the corresponding abbreviation (Desig.)) adopted in subsequent figures and tables. The number of sites is given by n. Climate is described by average ± standard deviation for latitude, Mean Annual Precipitation (MAP) and Mean Annual Temperature (MAT).

Plant Functional Type	Desig.	n	Latitude (°)	MAP (mm)	MAT (°C)
Non-tropical Broadleaf Forest	BL	17	44±7	850±294	10±4
Non-mediterranean Needleleaf Forest	NL	16	51±7	595±319	5±5
C3 Crop	Cr3	8	44±7	787±433	10±4
C4 Crop	Cr4	1	37±9	864±209	15±8
Tundra Shrub	Tu	2	69±1	158±231	-9±1
Tropical Broadleaf Forest	TBL	4	2±10	2150±631	27±2
C3 Grass	C3	14	43±8	651±383	10±6
C4 Grass	C4	4	-5±30	542±250	21±4
Non-tundra Shrub	SH	7	34±5	336±213	17±7
Mediterranean Needleleaf Forest	MNL	6	34±4	1370±572	16±4

Table 3: Main datasets adopted in the present study. Model input data also includes biophysical parameters for each PFT averaged from collated literature values (Alton & Bodin 2010). Note that the temporal resolution refers to the original dataset and does not necessarily correspond to that used either in the model simulations (3-hourly) nor in the analysis (weekly or annual). LAI, NEE, LE, SWC and PET refer, respectively, to Leaf Area Index, Net Ecosystem Exchange, Latent Energy heat flux, fractional Soil Water Content and Potential Evapo-Transpiration.

Purpose	Dataset	Source	Resolution		Reference
			Spatial	Temporal	
Model Input	LAI	MODIS	7 km	8-day	Schaaf et al. (2002)
	Main Met.	FLUXNET	<1 km	$\sim$ hourly	Falge et al. (2002)
	Gap-filling Met.	Princeton	1°	3hr	Sheffield et al. (2006)
	Soil composition	FLUXNET	<1 km	singular	Agarwal (2012)
Validation	NEE, LE	FLUXNET	<1 km	$\sim$ hourly	Falge et al. (2002)
	SWC1, SWC2	FLUXNET	<1 km	$\sim$ weekly	Falge et al. (2002)
	PET	Princeton	1°	annual	Sheffield et al. (2012)

Table 4: Root-mean square error (RMSE) in simulated Net Ecosystem Exchange at light saturation (NEE(sat)) and fractional soil water content (SWC2). Averaging is over weekly values for all siteyears comprising any given PFT. Designation for PFT follows Tab. 2. RMSE is shown separately for each model (JULES-def, JULES-tap, JULES-tap-HR). No SWC2 measurements are available for C4 crops, tundra and shrubs.

PFT	RMSE(NEE(sat)) [μmol m^{-2} s^{-1}]			RMSE(SWC2) [-]		
	JULES-def	JULES-tap	JULES-tap-HR	JULES-def	JULES-tap	JULES-tap-HR
BL	3.60	2.87	2.76	0.108	0.090	0.093
NL	2.31	2.02	2.19	0.063	0.060	0.085
Cr3	10.92	8.24	7.01	0.099	0.077	0.108
Cr4	2.64	3.13	3.65	–	–	–
Tu	0.12	0.06	0.10	–	–	–
TBL	7.77	5.23	4.75	0.130	0.110	0.096
C3	3.34	4.51	4.58	0.043	0.031	0.055
C4	14.05	12.99	14.61	0.039	0.044	0.033
SH	4.35	1.07	0.74	–	–	–
MNL	2.33	1.50	1.57	0.065	0.052	0.061

Figure Captions:

Fig.1: Schematic of JULES hydrology. Soil moisture content (kg m^{-2}) within each of n soil layers (SMC(n); n=4) is determined by the balance between water input (precipitation (PPT)) and water output (Evapotranspiration (ET) and Runoff (RUN)), as well as changes in two smaller reservoirs (SNOW and CAN). ET consists of transpiration (TR) and evaporation from soil and plant surfaces (ES). Soil depths (m) are given to the left of the depicted soil and root system. Dashed lines denote potential water flow between vertically adjacent soil layers.

Fig.2: Observed (solid line) and modelled (dashed line) weekly Net Ecosystem Exchange (NEE) against modelled deficit of soil water content (ΔSWC). For any given site, ΔSWC is the maximum value simulated for that site (approximately field capacity) minus the SWC in any given week. For NEE, we average fluxes into bins of 1 week and then average weekly bins from the same PFT into bins of ΔSWC. Model results pertain to the default model (JULES-def). Profiles above zero correspond to nighttime exchange (NEE(night)) whilst negative profiles refer to NEE at light saturation (NEE(sat)). Panel labels follow the PFT designation in Tab. 2. For tundra (Tu) insufficient data are available to create a profile.

Fig.3: As Fig.2 but plotting for JULES-tap. Note that ΔSWC is a modelled variable. Therefore, both observed and modelled NEE span a different range in ΔSWC compared to Fig.2.

Fig.4: Gross Primary Product (GPP) plotted against Plant Available Water (PAW) averaged over weekly bins as in Fig. 2. GPP is given under canopy light saturation as values inferred from observed carbon fluxes (obs) and from the JULES-def (def) and JULES-tap (tap) simulations.

Fig.5: Change in Root-Mean Square Error (ΔRMSE) between the default and the tap root simulations (JULES-tap minus JULES-def). RMSE is calculated for a given site using all NEE fluxes recorded across all relevant siteyears and represents the difference between observed and modelled fluxes. ΔRMSE is plotted against the corresponding annual Potential Evapo-Transpiration (PET). The plot is produced using all sites with available NEE measurements with rejection of three 2σ outliers (n=59). The solid line shows the best linear fit.

Fig.6: Relative histogram of tap root fraction for individual sites retrieved from the model optimisation (n=79).

Fig.7: Observed (panel a) and modelled (panels b and c) fractional soil water content at average depths of 8 cm (SWC1) and 19 cm (SWC2). Points are pooled for all siteyears and PFTs for which observations are available and represent median weekly averages for each siteyear.

Fig.8: Observed (solid line) and modelled (dashed line: JULES-tap) fractional soil water content at depth 19 cm (SWC2) against week of the year. The graphs uses the corresponding points in Fig. 7 mean-averaged over each PFT. PFT designation follows Tab. 2.

Figure 1: Schematic of JULES hydrology. Soil moisture content (kg m^{-2}) within each of n soil layers (SMC(n); n=4) is determined by the balance between water input (precipitation (PPT)) and water output (Evapotranspiration (ET) and Runoff (RUN)), as well as changes in two smaller reservoirs (SNOW and CAN). ET consists of transpiration (TR) and evaporation from soil and plant surfaces (ES). Soil depths (m) are given to the left of the depicted soil and root system. Dashed lines denote potential water flow between vertically adjacent soil layers.

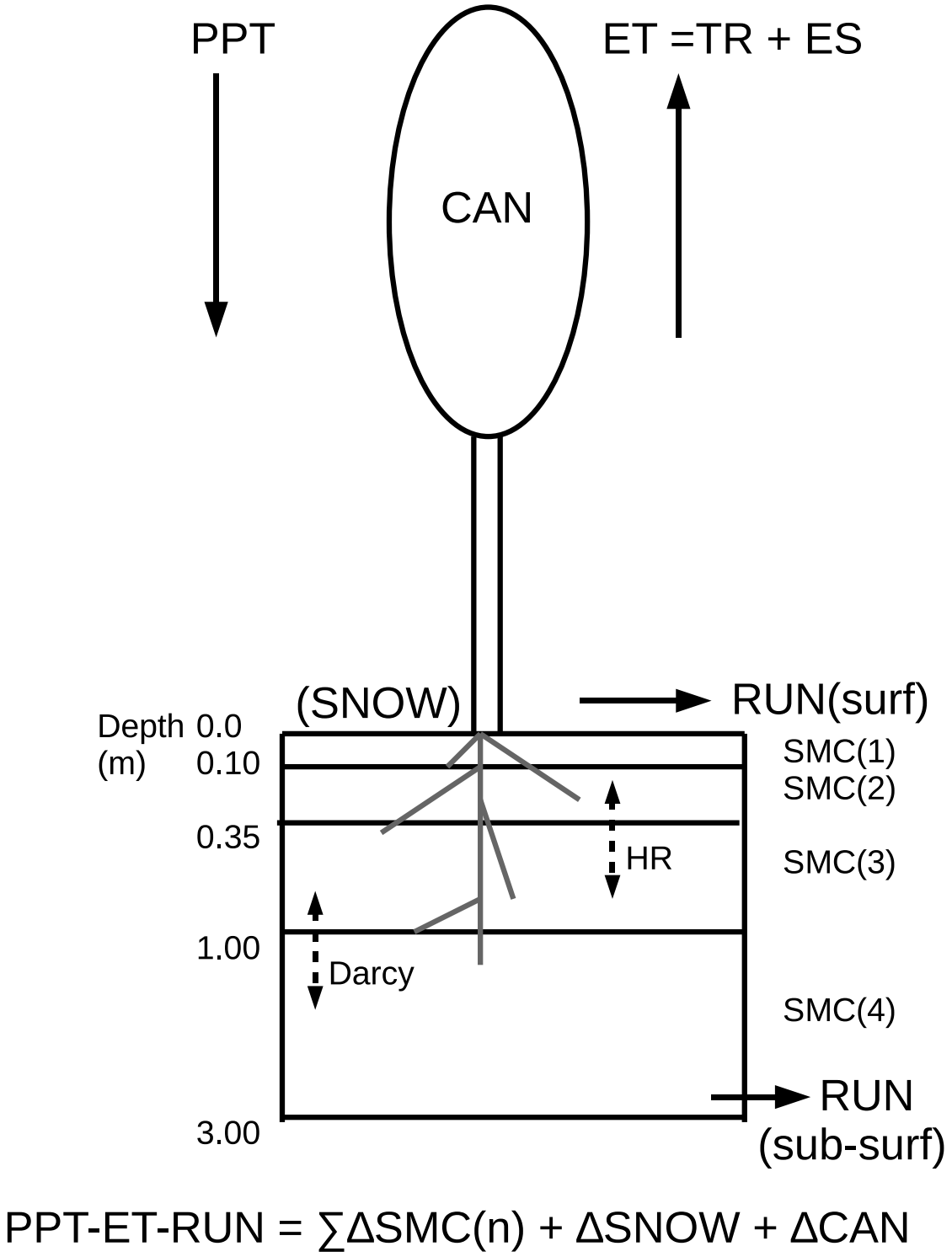

$$PPT\text{-}ET\text{-}RUN = \sum \Delta SMC(n) + \Delta SNOW + \Delta CAN$$

Figure 2: Observed (solid line) and modelled (dashed line) weekly Net Ecosystem Exchange (NEE) against modelled deficit of soil water content (ΔSWC). For any given site, ΔSWC is the maximum value simulated for that site (approximately field capacity) minus the SWC in any given week. For NEE, we average fluxes into bins of 1 week and then average weekly bins from the same PFT into bins of ΔSWC. Model results pertain to the default model (JULES-def). Profiles above zero correspond to nighttime exchange (NEE(night)) whilst negative profiles refer to NEE at light saturation (NEE(sat)). Panel labels follow the PFT designation in Tab. 2. For tundra (Tu) insufficient data are available to create a profile.

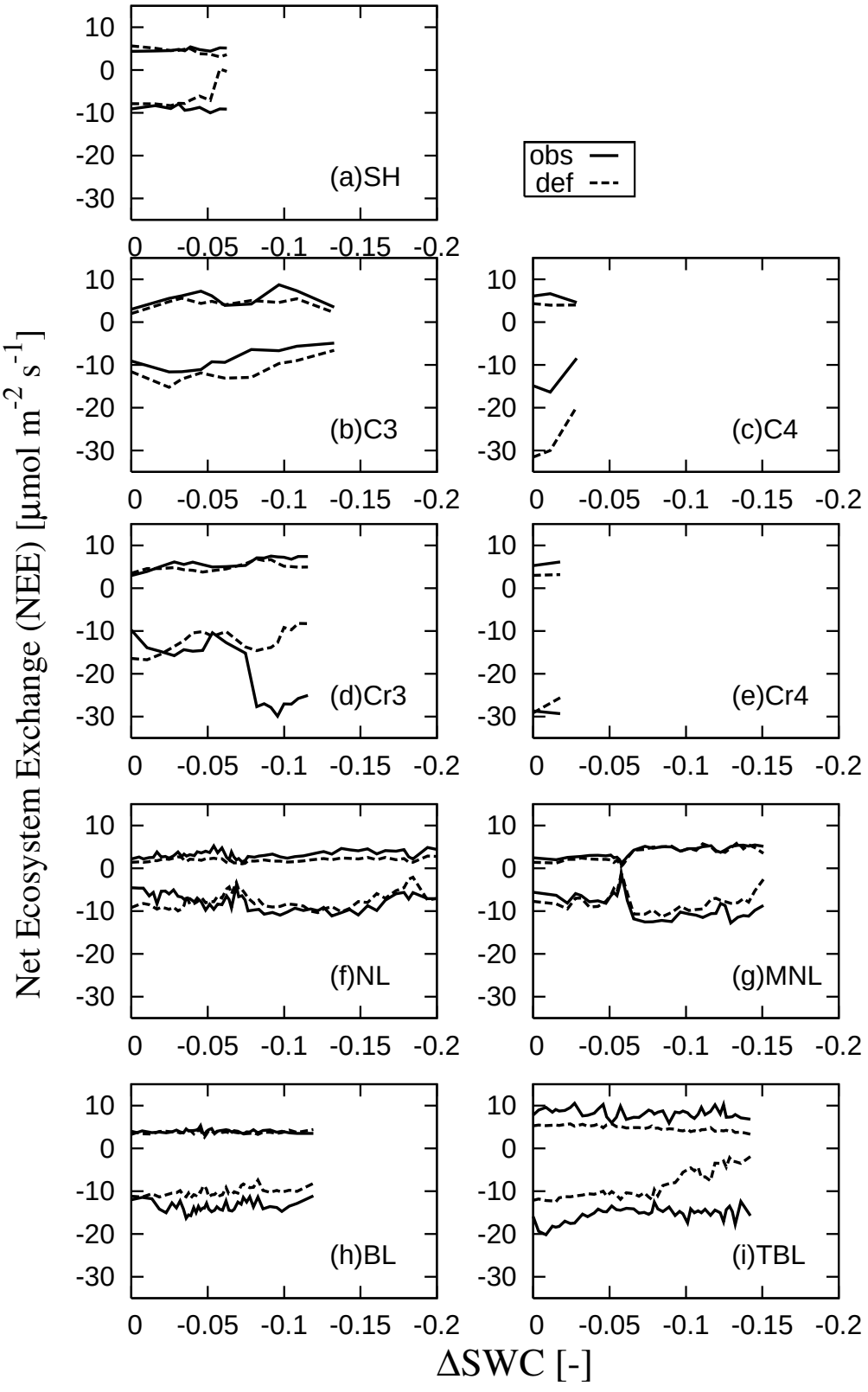

Figure 3: As Fig.2 but plotting for JULES-tap. Note that ΔSWC is a modelled variable. Therefore, both observed and modelled NEE span a different range in ΔSWC compared to Fig.2.

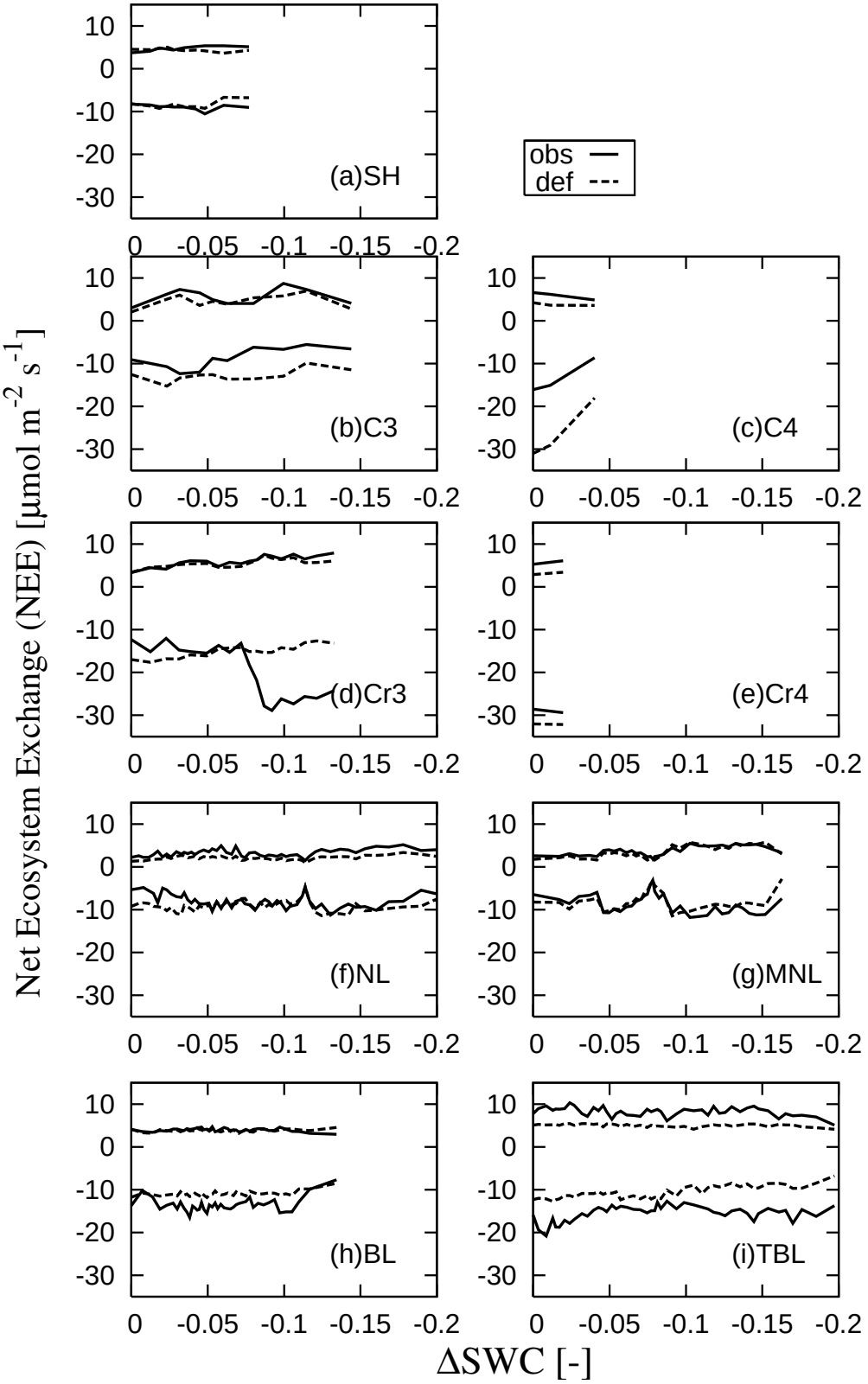

Figure 4: Gross Primary Product (GPP) plotted against Plant Available Water (PAW) averaged over weekly bins as in Fig. 2. GPP is given under canopy light saturation as values inferred from observed carbon fluxes (obs) and from the JULES-def (def) and JULES-tap (tap) simulations.

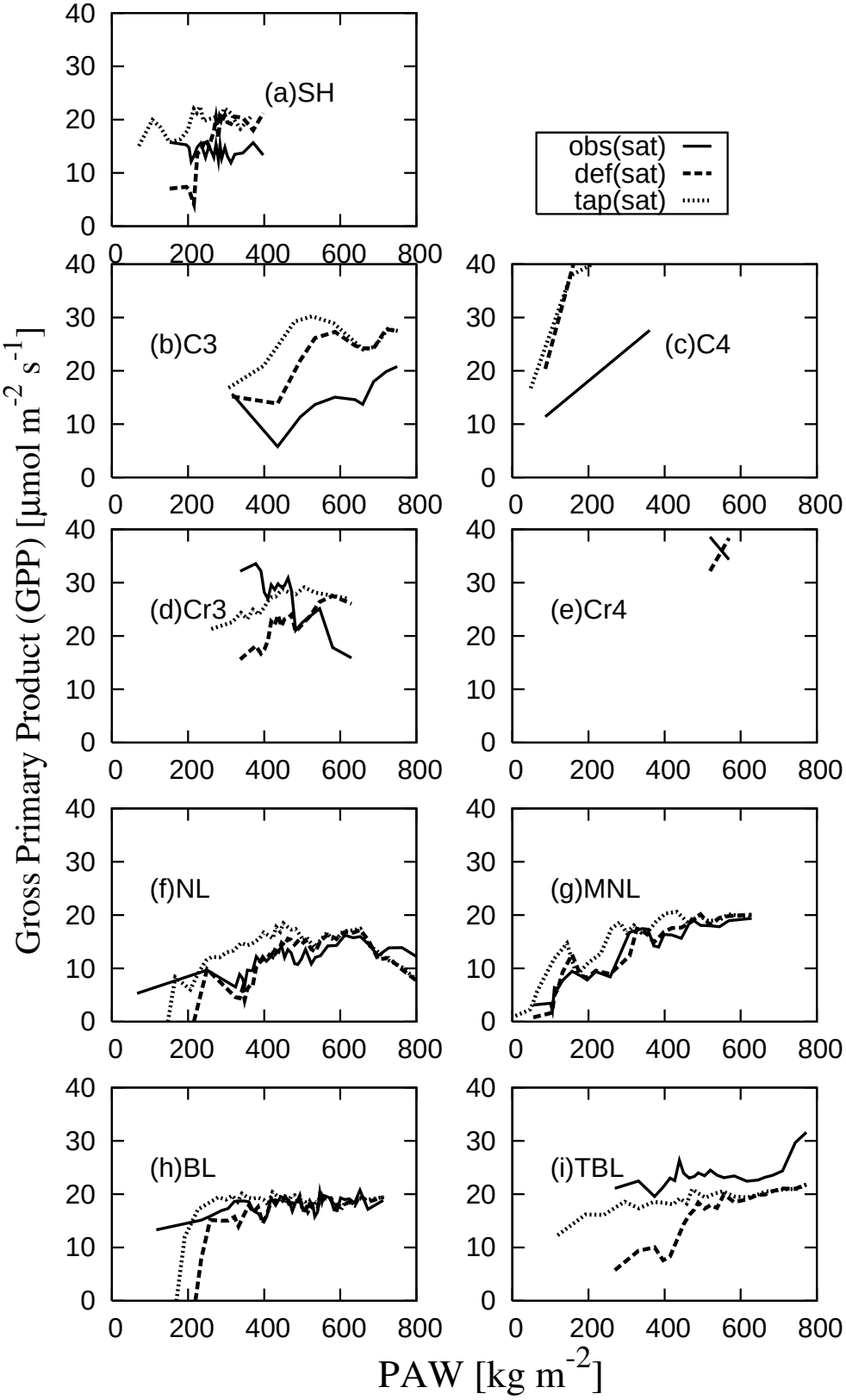

Figure 5: Change in Root-Mean Square Error (ΔRMSE) between the default and the tap root simulations (JULES-tap minus JULES-def). RMSE is calculated for a given site using all NEE fluxes recorded across all relevant siteyears and represents the difference between observed and modelled fluxes. ΔRMSE is plotted against the corresponding annual Potential Evapo-Transpiration (PET). The plot is produced using all sites with available NEE measurements with rejection of three 2σ outliers (n=59). The solid line shows the best linear fit.

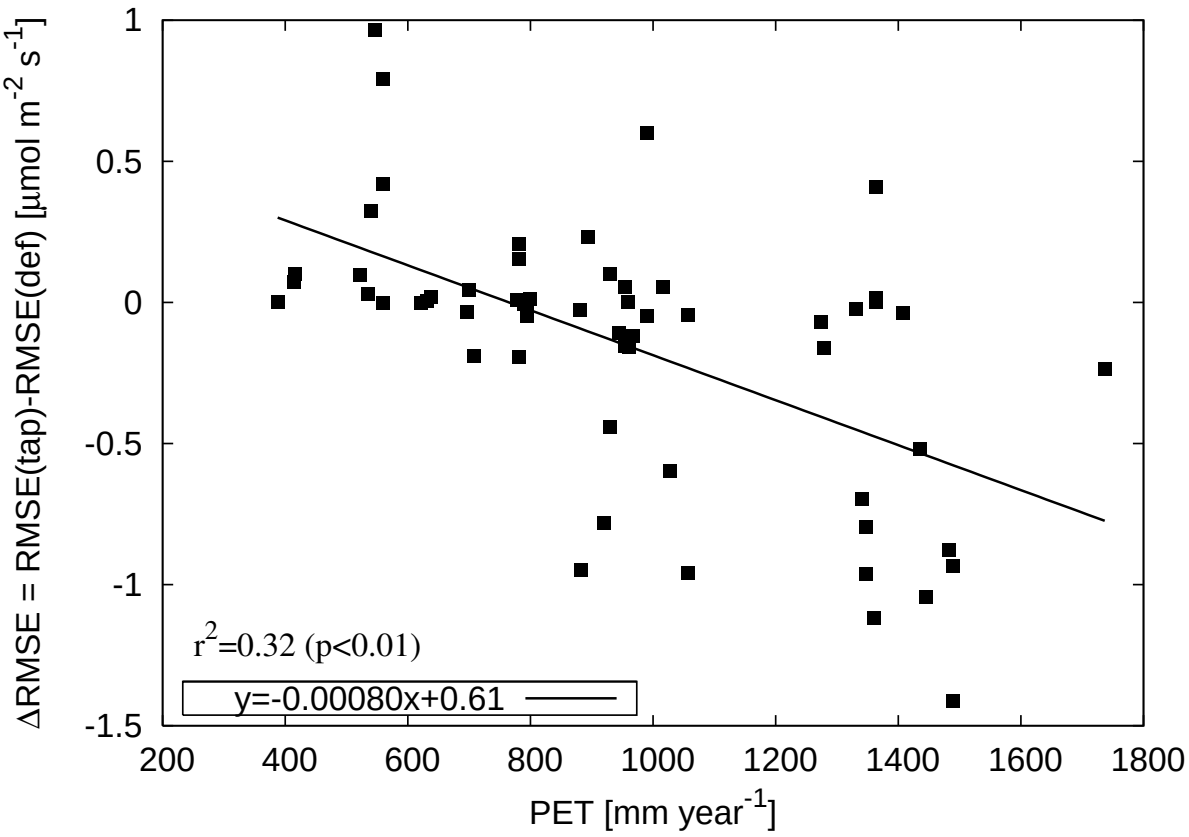

Figure 6: Relative histogram of tap root fraction for individual sites retrieved from the model optimisation (n=79).

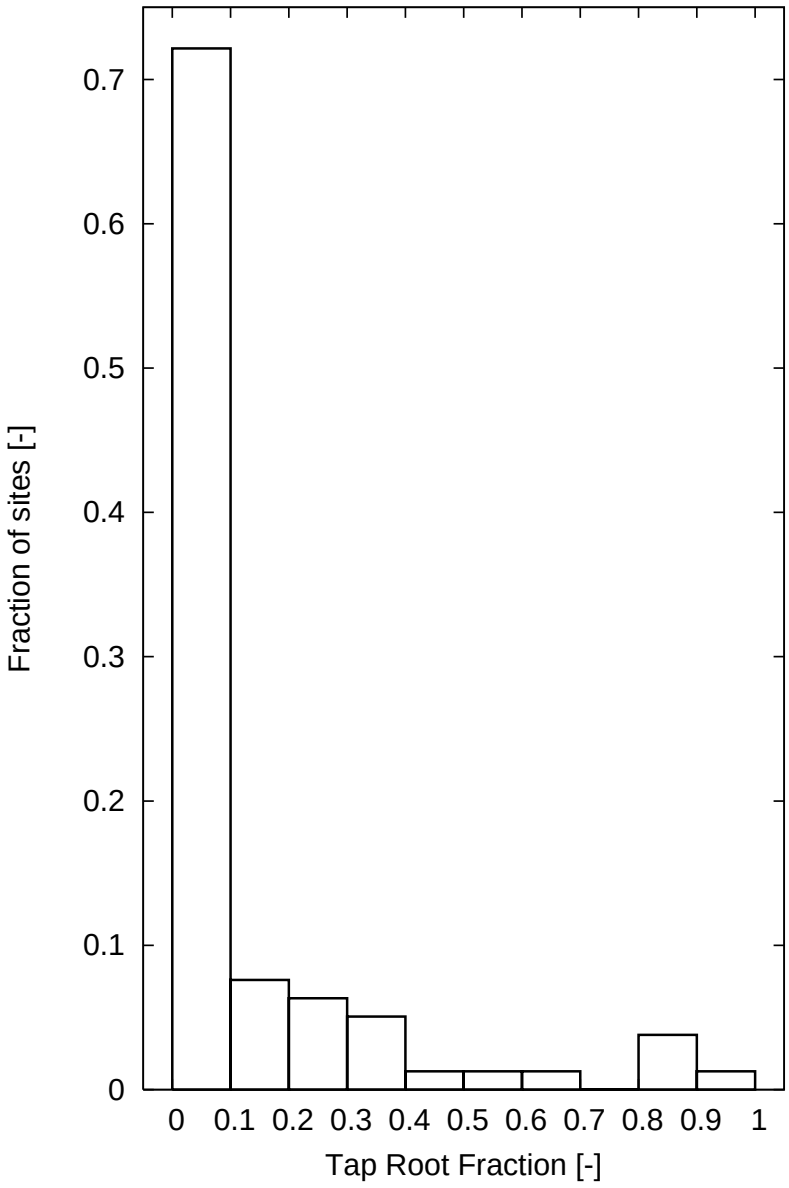

Figure 7: Observed (panel a) and modelled (panels b and c) fractional soil water content at average depths of 8 cm (SWC1) and 19 cm (SWC2). Points are pooled for all siteyears and PFTs for which observations are available and represent median weekly averages for each siteyear.

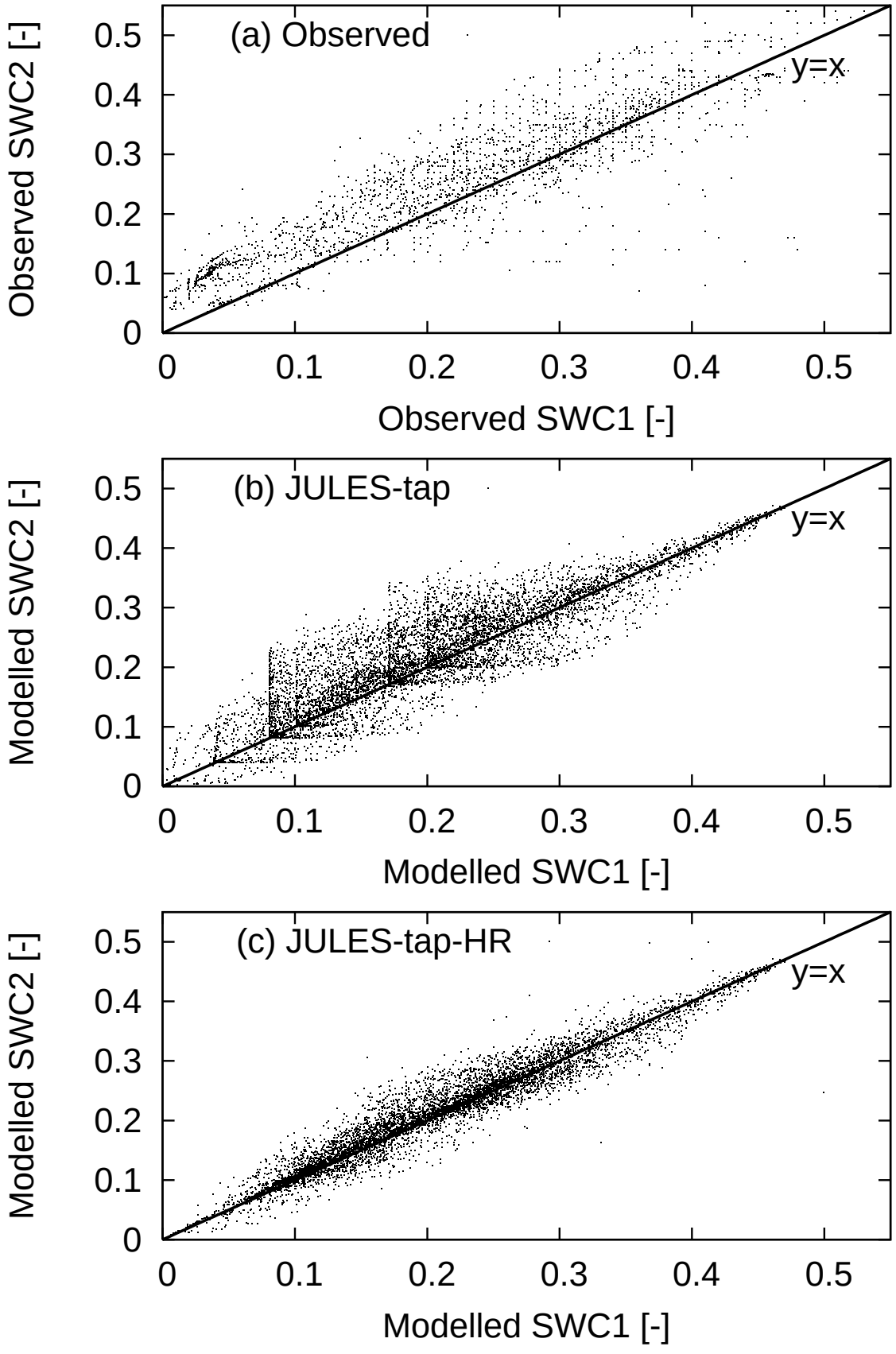

Figure 8: Observed (solid line) and modelled (dashed line: JULES-tap) fractional soil water content at depth 19 cm (SWC2) against week of the year. The graphs uses the corresponding points in Fig. 7 mean-averaged over each PFT. PFT designation follows Tab. 2.